

Cell Reports, Volume 30

Supplemental Information

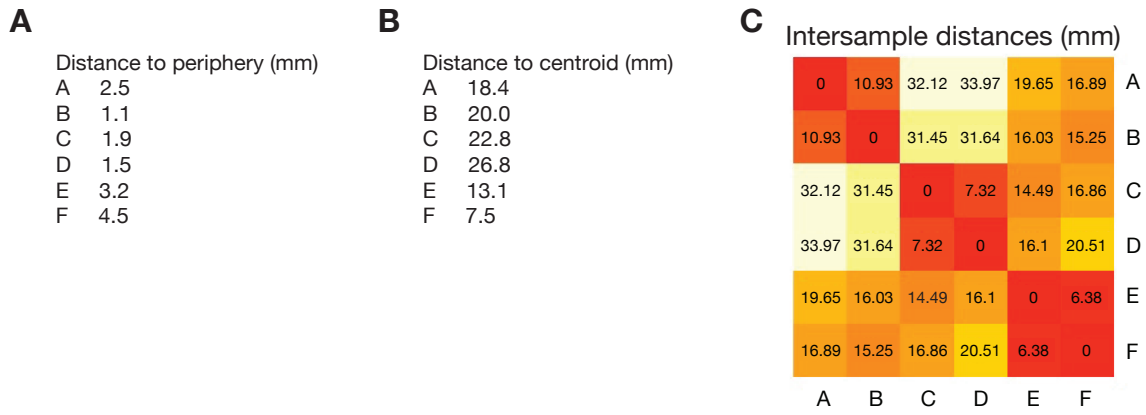
Multiplatform Molecular Profiling

Reveals Epigenomic Intratumor

Heterogeneity in Ependymoma

S. John Liu, Stephen T. Magill, Harish N. Vasudevan, Stephanie Hilz, Javier E. Villanueva-Meyer, Sydney Lastella, Vikas Daggubati, Jordan Spatz, Abrar Choudhury, Brent A. Orr, Benjamin Demaree, Kyounghee Seo, Sean P. Ferris, Adam R. Abate, Nancy Ann Oberheim Bush, Andrew W. Bollen, Michael W. McDermott, Joseph F. Costello, and David R. Raleigh

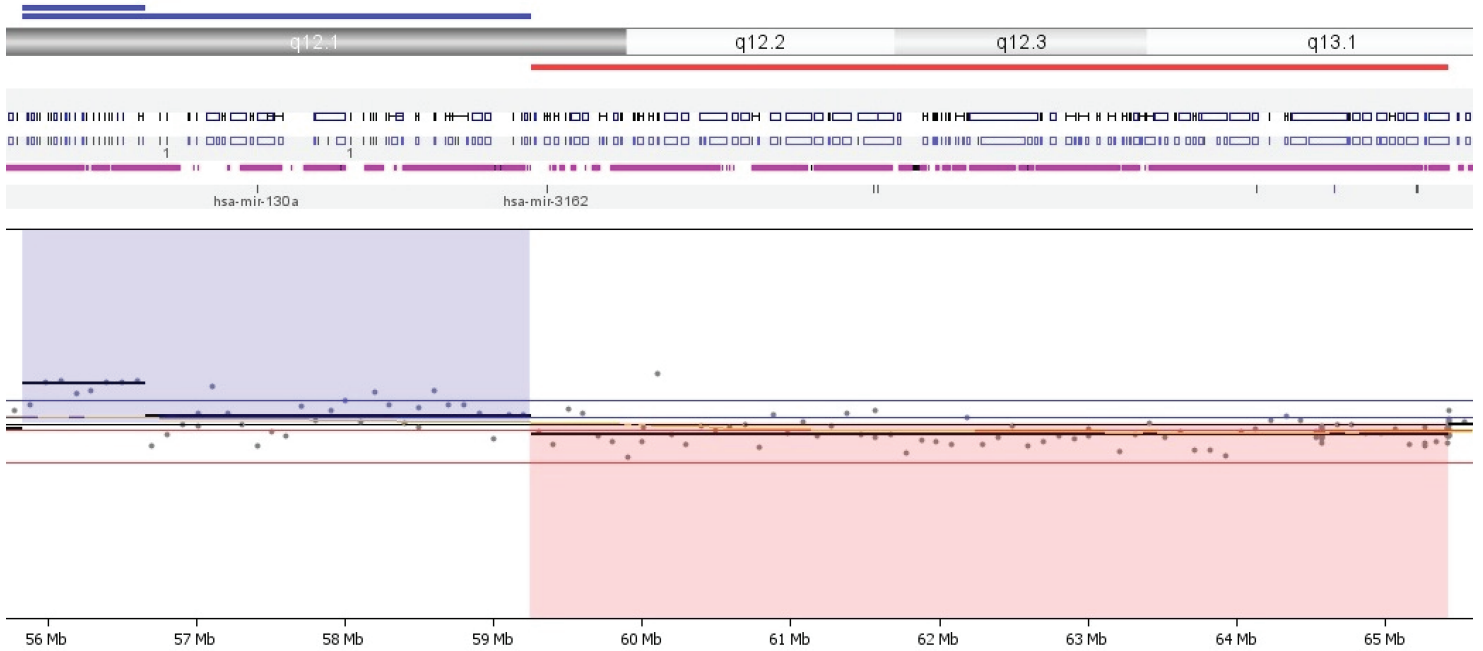
Figure S1, Related to Figure 1. Stereotactic mapping of an anaplastic ependymoma with C11orf95-RELA fusion.



(A, B) Spatial mapping of tumor contour with defined sample coordinates in relation to the tumor periphery (A) and tumor centroid (B) measured in millimeters. (C) Pairwise distance matrix between samples measured in millimeters.

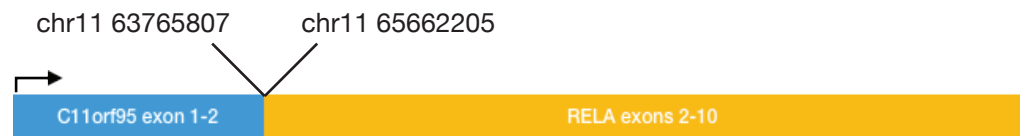
Figure S2, Related to Figure 2. Genomic and radiologic characterization of an anaplastic ependymoma with C11orf95-RELA fusion.

A

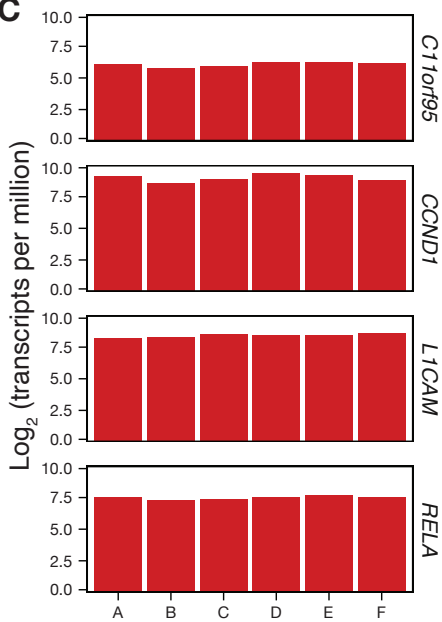


B

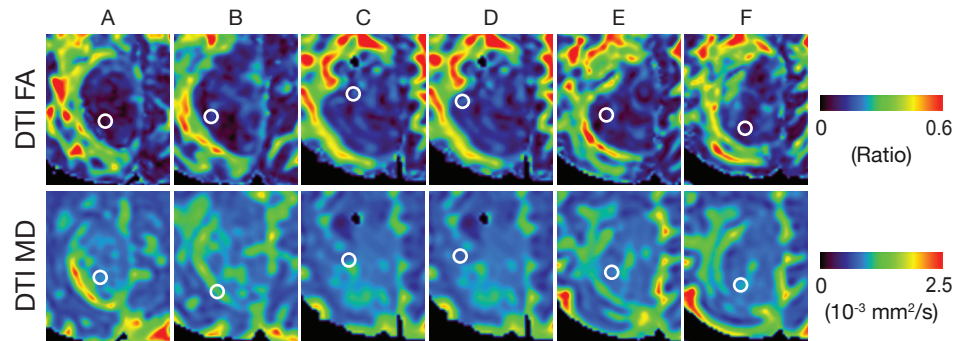
Fusion detector	Reads
JAFFA	26
Tophat Fusion	24



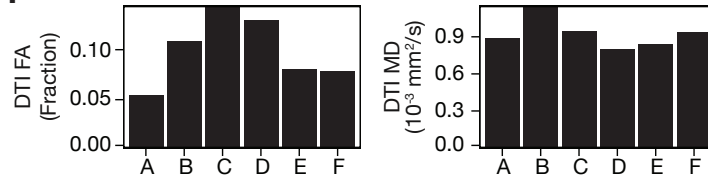
C



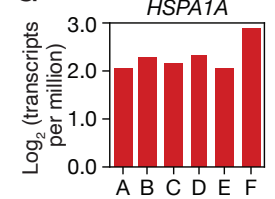
E



F



G

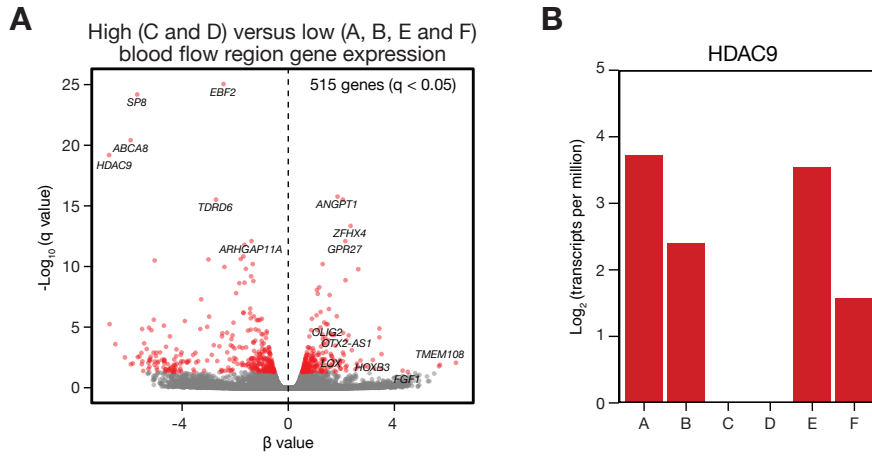


D



(A) Segmental chromosome 11q deletions and amplifications detected on targeted DNA sequencing, consistent with chromothripsis. (B) Number of exon junction spanning reads supporting C11orf95-RELA fusion as detected by JAFFA and Tophat Fusion (left), and gene fusion schematic with hg38 genomic coordinates (right). (C) Expression of ependymoma markers from RNA-seq reveals uniform enrichment of C11orf95-RELA target genes across samples. (D) Gene ontology analysis shows distinct enrichment patterns of stem-like, neuronal fate specification and immune signaling genes in stereotactic samples. (E, F) Quantitative MRI measurements of stereotactically-defined regions demonstrates enhanced fractional anisotropy in samples with stem-like identity (C and D). White circles indicate stereotactic sample locations. DTI, diffusion tensor imaging; FA, fractional anisotropy; MD, mean diffusivity; MRI, magnetic resonance imaging. (G) RNA-seq expression of the hypoxia gene HSPA1A across samples shows enrichment in sample F, the sample closest to the tumor centroid.

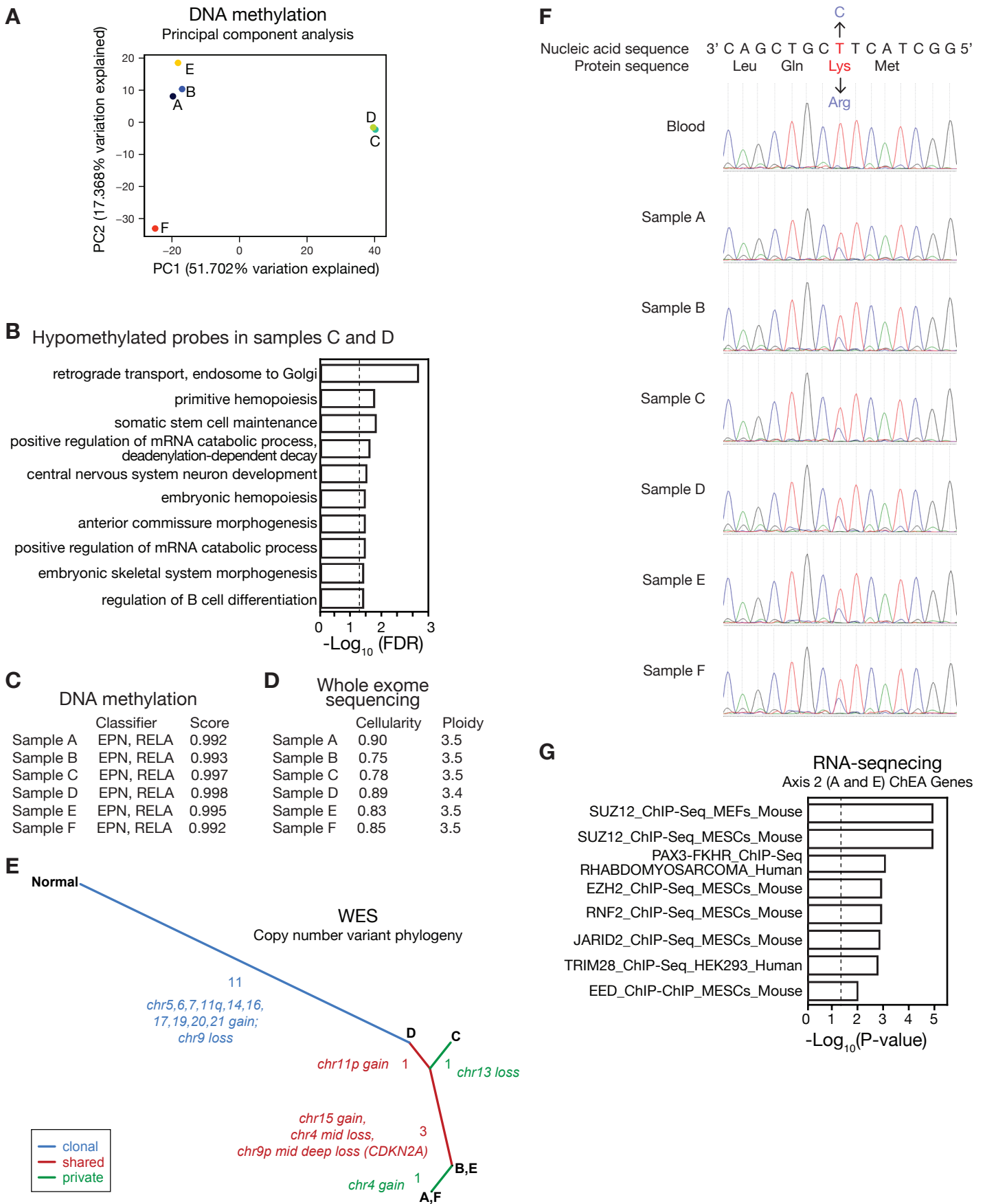
Figure S3, Related to Figure 2. Differences in cerebral blood flow drive intratumor heterogeneity within an anaplastic ependymoma with C11orf95-RELA fusion.



(A) Differential RNA-seq expression analysis of high versus low blood flow regions reveals 515 significantly expressed genes.

(B) RNA-seq expression of the histone deacetylase gene HDAC9 across samples shows depletion in samples C and D, the samples with the highest blood flow.

Figure S4, Related to Figure 3. Intratumor heterogeneity within an anaplastic ependymoma with C11orf95-RELA fusion.



(A) PCA of DNA methylation profiles reveals 69% percent of variation is explained by the first two principal components (PC). (B) Genomic Regions Enrichment of Annotations Tool (GREAT) gene ontology analysis of hypomethylated probes in samples and D is consistent with expression of stem cell genes. (C) DNA methylation profile based classification reveals RELA ependymoma in each sample (Capper et al., 2018). (D) Cellularity and ploidy results from Sequenza analysis demonstrates equivalent tumor composition in each sample. (E) Intratumor phylogeny based on clonal ordering of copy number variants derived from exome sequencing suggests that chromosomal structural alterations are an early event during ependymoma tumorigenesis. The number and identify of copy number variants defining each axis are indicated. (F) Sanger sequencing of SETD2 exon 1 reveals 5A>G (p.K2R) missense substitution in all tumor samples. (G) Chromatin Enrichment Analysis (ChEA) gene ontology of the top 200 genes in axis 2 from RNA-seq PCA shows enrichment for targets of SUZ12 and EZH2. Vertical dashed line corresponds to P=0.05.